TLR3 stimulation improves the migratory potency of adipose-derived mesenchymal stem cells through the stress response pathway in the melanoma mouse model

Fatemeh Eskandari
Iran University of Medical Sciences
Samira Zolfaghari
Iran University of Medical Sciences
Ayna Yazdanpanah
Iran University of Medical Sciences
Rima Manafi Shabestari
Iran University of Medical Sciences
Motahareh Rajabi Fomeshi
Iran University of Medical Sciences
Peiman B. Milan
Iran University of Medical Sciences
Jafar Kiani
Iran University of Medical Sciences
Mina Soufi Zomorrod
Tarbiat Modares University Faculty of Medical Sciences
Majid Safa (majidsafa@gmail.com)
Iran University of Medical Sciences

Research Article

Keywords: adipose-derived mesenchymal stem cells (ADMSCs), toll-like receptor 3 (TLR3), stress response, tumor tropism, melanoma mouse model

Posted Date: July 21st, 2022

DOI: https://doi.org/10.21203/rs.3.rs-1842096/v1

Version of Record: A version of this preprint was published at Molecular Biology Reports on December 28th, 2022. See the published version at https://doi.org/10.1007/s11033-022-08111-8.

Abstract

Background

Mesenchymal stem cells (MSCs) are utilized as a carrier of anti-tumor agents in targeted anti-cancer therapy. Despite the improvements in this area, there are still some unsolved issues in determining the appropriate dose, method of administration, biodistribution, and long-term survival. The current study aimed to determine the influence of toll-like receptor 3 (TLR3) stimulation on the potential of MSCs migration to the neoplasm environment in the mouse melanoma model.

Methods and Results

Adipose-derived MSCs (ADMSCs) were isolated from the GFP^+ transgenic C57BL/6 mouse and treated with different doses (1μg/ml and 10 μg/ml) of polyinosinic-polycytidylic acid [poly(I:C)], the related TLR3 agonist, at various time points (1 and 4 hours). Following the treatment, the expression pattern of targeted genes such as α4, α5, and β1 integrins and TGF-β and IL-10 anti-inflammatory cytokines was determined using real-time PCR. In vivo live imaging evaluated the migration index of the intraperitoneally (IP) injected treated ADMSCs in a lung tumor-bearing mouse (C57BL/6) melanoma model (n = 5). The presented findings demonstrated that TLR3 stimulation led to enhanced migration of ADMSCs to the tumor area compared with control group (n = 5) and enhanced expression of α4, α5, and β1 integrins. It was also detected that the engagement of TLR3 resulted in the anti-inflammatory behavior of the cells, which might influence the directed movement of ADMSCs.

Conclusions

This research identified that TLR3 activation might improve the migration via the stimulation of stress response in the cells and depending on the agonist concentration and time exposure, these activated pathway drive the migratory behavior of MSCs.

1. Introduction

Cell-based therapy with mesenchymal stem cells (MSCs) has been considered a key approach in regenerative medicine and many clinical situations [1–3]. Because of the various promising features of MSCs like multilineage differentiation capability [4], easy isolation from the multitude of sources [5, 6], migration to the damaged area [7, 8] and, also immunomodulatory responses [9], there has been increasing consideration in taking advantages of these cells in therapeutic applications.

MSCs also have been proven to be employed in targeted anti-cancer therapy as a carrier of anti-tumor drugs due to their innate tropism to the neoplasm areas [10–12]. The tumor microenvironment, an “unhealed wound,” can induce MSCs migration because of its typical inflammatory state comparable to

the injured site [13]. This MSCs feature is undertaken in stress conditions such as mechanical injury (wounds), inflammation, infection, or cancer. Even though the mechanism of MSCs tumor tropism is unknown, the trans-endothelial migration of MSCs toward tumors is comparable to that of leukocytes, including processes such as rolling, adhesion, and extravasation. Consequently, it makes the MSCs egress from their niche and allows them to migrate into the circulation, invade vessels, and engraft the injured site to perform their repair function [14]. Some evidence supports the involvement of inflammatory signals in cancer as environmental cues in MSCs migration and biodistribution paradigm [15]. Previous research has shown that reducing tumor load and extending the lifespan of animal studies of melanoma, lung, breast cancer, and glioma using MSC expressing IL-12, interferon-β (IFN-β), and prodrugs [16–18].

While advancement in MSC-based therapy in treating numerous pathologic conditions and improving the quality of life, there remain some unclear challenges in establishing optimal dosage, route of administration, determination of their biodistribution, long-term viability, and biological fate [19]. Developing strategies to achieve the desired therapeutic efficacy for future practical MSCs application is required. Many findings have proposed that the preconditioning of MSCs using various factors in different conditions, including inflammatory cytokines [20, 21], hypoxic preconditioning [22, 23], Toll-like receptors (TLRs)-ligand priming [24], can enhance the migratory and homing behavior of these cells.

TLRs are a family of conserved receptors that identify pathogen-associated molecular patterns (PAMPs) and damaged-associated molecular patterns (DAMPs) and induce immune cell activation. TLR agonist activation induces the production of inflammatory cytokines or co-stimulatory molecules through the myeloid differentiation primary response 88 (MyD88)-dependent or MyD88-independent signaling pathway, which may increase the stimulated cell's chemotaxis [25–27].

Numerous reports have investigated MSCs as cells that express TLRs. According to previous findings on mesenchymal and hematopoietic stem cells, TLRs engagement may function in stem cell biology, particularly enhancing their migratory ability. As a critical factor in innate immune response, TLRs have been introduced to drive MSC homing by regulating a range of chemokine receptors such as CXC and CC receptors and activating integrins and other adhesion molecules involved in cell migration. As a result, TLR activation might be one strategy that promotes MSC recruitment and migration in wounded or stressed regions [28–31]. The discovery of TLRs as essential mediators of stress responses inside MSCs establishes a new component of their biology. It gives a unique target for improving stem cell-based treatment technics.

Previous studies did not investigate the involvement of TLR3 in significant migratory responses of stem cells in a tumor model, which we are focusing on here. In the current study, relying on the TLR-ligand-activated pathway, we aimed to determine whether TLR3 stimulation influences the potential of MSCs migration and recruitment to the neoplasm environment in a melanoma mouse model.

2. Materials And Methods

2.1. Adipose-derived MSCs (ADMSCs) preparation and culture

Using collagenase type I digestion protocol [32], ADMSCs were prepared from 6–8 weeks male C57BL/6 GFP-transgenic mice (purchased from Stem Cell Technology Research Center, Tehran, Iran) abdominal fat. Briefly, after cervical dislocation of the animal, isolated abdominal fat was collected in sterile condition and washed with phosphate buffer saline (PBS) (Sigma-Aldrich, St. Louis, Missouri, USA) containing 1% penicillin/streptomycin antibiotic (Sigma-Aldrich; St. Louis, Missouri, USA). After that, samples were cut into small pieces and then digested with 0.075% collagenase type I (Gibco, Waltham, Massachusetts, USA) diluted in Dulbecco's Modified Eagle's Medium-high glucose (DMEM), (Sigma-Aldrich, St. Louis, Missouri, USA) without fetal bovine serum (FBS) (Gibco, Waltham, Massachusetts, USA) for 30 minutes at 37°C cell culture incubator [33]. The digestive process was neutralized by adding an appropriate volume (5 ml) of DMEM high glucose supplemented with 10% heat-inactivated FBS and centrifuged for 15 minutes at 300 g. Cellular pellet was resuspended and washed two times under the same previous condition to remove undigested tissues. Finally, the cellular pellet was resuspended and cultured in tissue culture flasks in a complete cell culture medium consisting of high glucose concentration containing 10% FBS, 2 mmol/L l-glutamine (Sigma-Aldrich, St. Louis, Missouri, USA), and 1% penicillin/streptomycin at 37°C with 5% CO_2 humidified incubator [34]. The medium was replaced with a fresh medium to remove non-adherent cells after 72 hours of starting culture. The fibroblast-like appearance of the cells isolated from fat was confirmed by an inverted microscope (Zeiss, Jena, Germany). After reaching the 80% confluency, the cells were passaged using 0.25% Trypsin/0.02% EDTA (Gibco, Waltham, Massachusetts, USA) for further expansion. ADMSCs were used for two weeks expansions at passages 2–3 for all experiments to maintain consistency.

2.2. Immunophenotyping of ADMSCs

Flow cytometry was used to validate the MSCs phenotype, which was determined by the presence of CD105, CD90, and CD73 antigens in the lack of CD45, CD34 antigens using purchased antibodies (BD Biosciences (San Diego, CA, USA)). According to the standard protocol, the surface staining of the cells was performed, and samples were characterized using a FACScan flow cytometer (Becton Dickinson, Franklin Lakes, New Jersey, USA). The flow Jo software (Ashland, Oregon, USA) was used to analyze the data.

2.3. Preconditioning of TLR3

TLR3 preconditioning of ADMSCs was performed using poly(I:C) (1 μg/mL, 10 μg/mL) (Sigma-Aldrich, St. Louis, Missouri, USA) as the agonist. 5×10^4 cells were seeded in 24 well plates per well to reach 70–80% confluency. After that, the culture medium was removed, and the cells were washed with PBS and treated using poly(I:C) prepared in a complete culture medium for 1 and 4 hours for all mentioned concentrations. The control cells were incubated with only a complete medium. After incubation time

points, cells were washed with PBS three times and incubated in a complete medium for further experiments.

2.4. Cell proliferation assay

MTT (3-(4,5-dimethyl thiazolyl-2)-2,5-diphenyl tetrazolium bromide) (Sigma-Aldrich, St. Louis, Missouri, USA) was utilized to monitor the cell growth. MSCs are pre-conditioned under a variety of settings, as previously stated. After that, each control and poly(I:C)-pre-treated cell received 500 µl of 5 mg/ml MTT solution 24 hours, 48 hours, and 72 hours after treatment. After a 4 hours incubation period, the medium was sucked off, and the crystals of formazan were dissolved in 150 µl dimethyl sulfoxide (DMSO) (Merck, Readington, New Jersey, USA). The absorption spectrum at 570 nm was measured using an ELISA plate analyzer. Samples were examined in triplicate in this investigation.

2.5. RNA purification and quantitative real-time PCR

Following the manufacturer's instruction, the TriPure isolation reagent (Roche, Basel, Switzerland) was used to isolate the total RNA after priming the cells with poly(I:C). A NanoDrop 2000 spectrophotometer (Thermo Scientific, Waltham, Massachusetts, USA) was used to quantify RNA concentration, and the DNA decontamination process with a DNase kit (Thermo Scientific, Waltham, Massachusetts, USA) eradicated any potential DNA contamination in the RNA sample. After then, cDNA was made from 1µg of RNA using a RevertAid First Strand cDNA Synthesis kit (Thermo Scientific, Waltham, Massachusetts, USA). The Rotor-Gene 6000 Real-Time PCR System (Corbett Research, Hilden, Germany) was used to perform the test using the Maxima SYBR green master mix (Fermentas, Waltham, Massachusetts, USA). Denaturation at 95°C for 15 seconds and annealing and elongation at 60°C for 60 seconds was used to amplify DNA in a 40-cycle PCR reaction. The fold change was computed compared to the untreated control cells after correcting for the TATA-Box binding protein (TBP) reference gene. Relative gene expression levels were calculated utilizing the $2^{-\Delta\Delta Ct}$ method [33]. Representative data sets are provided for each sample examined in triplicate. The following are the primer sequences: (Table 1. Primer sequences for qRT-PCR).

Table 1
Primer sequences used in real-time PCR

Primer Name	Oligo Sequences 5'→3'	Tm (˚C)	Size (bp)
TBP-F	TTGGGCTTCCCAGCTAAGTTC	60.27	21
TBP-R	TCTGGCTCATAGCTACTGAACTG	59.62	23
TGF-β-F	CGCAACAACGCCATCTATGAG	60.00	21
TGF-β-R	TCTGCACGGGACAGCAATG	60.67	19
IL-10-F	GACAATAACTGCACCCACTTCC	59.51	22
IL-10-R	CTGCATTAAGGAGTCGGTTAGC	59.13	22
α4-Integrin-F	GAAGGCAGAGTCTCCGTCAAG	60.40	21
α4-Integrin-R	GATGTCTCGCACGTCTTTCC	59.01	20
α5-Integrin-F	CTATCCAGTGCACCACCATTC	58.71	21
α5-Integrin-R	TTTCTGTGCGCCAGCTATAC	58.35	20
β1-Integrin-F	CGAGGTCGTTCAGTTCATC	57.79	19
β1-Integrin-R	TGTCTTCACTGTTCACTTCATCTGT	60.40	25

2.6. Transwell migration/invasion assay

For invasion assay, pre-treated ADMSCs were plated in Matrigel (Corning, New York, USA) pre-coated 24-well transwell inserts with 8.0 μm pore membrane filters (Corning, New York, USA). Briefly, the insert's filters were coated with diluted Matrigel to imitate the basement membrane and then incubated for 24 hours at 37°C. Pre-conditioned and untreated MSCs were seeded on the upper chamber of inserts (10^4 cells in 250μl serum-free culture medium). 5×10^4 B16-F10 melanoma cells were plated in the lower chamber of the transwell containing the 10% FBS culture medium. After 24 hours of incubation at 37°C and 5% CO_2, the upper chamber culture medium was removed and washed with PBS three times. The cells that reached the lower surface of the filter were fixed with methanol and stained with 2% crystal violet (Sigma-Aldrich, St. Louis, Missouri, USA) [35]. The migrated MSCs were detected using a microscope in 10X magnification (Zeiss, Jena, Germany), and the number of cells was determined using the ImageJ software (National Institutes of Health, USA) [36].

2.7. Western blot analysis

After preconditioning, the MSCs were rinsed with a cold PBS/phosphatase inhibitor/protease inhibitor cocktail (Sigma-Aldrich, St. Louis, Missouri, USA). Then the nuclear extract was made by adding 250 μl of hypotonic buffer to the 4×10^6 treated MSCs. The lysed cells were centrifuged at 14000 g for 1 minute at 4°C. The supernatant was removed, then the cellular pellet was resuspended in 50μl complete lysis buffer, protease/phosphatase inhibitor cocktail, and centrifuged at 14000 g for 15 minutes at 4°C. The

supernatant was collected, and protein concentration was measured by Bradford protein assay (Bio-Rad, Hercules, CA, USA).

Equal quantities of extracted nuclear fraction were separated on 10% SDS-PAGE. Then electro-transferred onto a nitrocellulose membrane (Hybond-ECL, Amersham Corp, UK) using a semidry transfer cell (Bio-Rad, Hercules, CA, USA) for subsequent immunoblotting. Membranes were then blocked for 1 hour at room temperature with 5% nonfat dry milk in TBS containing 0.1% (v/v) Tween-20 (TBST) prior to being analyzed with diluted specified primary antibodies (Amersham Pharmacia Biotech, United Kingdom) overnight at 4°C. The membranes were rinsed three times in TBST and then treated with horse radish peroxidase-conjugated (HRP) secondary antibodies. Then we used the chemiluminescence detection method to view the proteins (Amersham ECL Advance Kit, GE Healthcare, UK) [37]. ImageJ software (National Institutes of Health, USA) was used for densitometric quantification.

2.8. In vivo experiment

6–8 weeks male C57BL/6 mice were supplied from the Iran University of medical sciences, center for experimental and comparative studies. The animals were cared by the ethical principles of the National Institutes of Health Guide for the Care and Use of Laboratory Animals and approved by the ethics committee of the Iran University of Medical Sciences (Code of Ethics: IR.IUMS.REC.1397.1172). The experiment was repeated twice with 10 mice (5 mice for laboratory experiments and 5 for survival) in each group. Each mouse received 3×10^5 B16-F10 cells via tail vein injection to establish a melanoma tumor in the lung. Tumors formed in the lungs after 10 days. To verify the neoplasm formation in the lung, the small animal positron emission tomography scan (PETs) technic was employed with a micro-PET scanner (Xtrim PET) at the Preclinical Core Facility (TPCF) based at the Tehran University of Medical Sciences. The mice were injected through the tail vein with about 300 μCi of the 18FDG under general anesthesia. For each small animal PET scan, qualitative analysis was performed to examine the model or metastasis. Subsequently, after confirming the tumor establishment in the lungs, mice were intraperitoneally (IP) injected with 10^6 cells from two different GFP^+ ADMSC groups separately: untreated ADMSCs (n = 10) and poly(I:C)-treated ADMSCs (n = 10) (10μg/ml for 1hour treatment).

2.9. Assessment of ADMSCs homing

2.9.1. GFP tracking using live imaging

The in vivo imaging was performed using the KODAK imaging system (FX Pro, Rochester, New York, USA) with florescent mode and 5 min exposure time to track the localization of GFP^+ ADMSCs 3, 10, and 14 days after IP injection (n = 5 in each group). The excitation and emission filters were set to 470 nm and 535 nm, respectively. The light emitted from the mice was captured, integrated, processed, and displayed by the KODAK camera system. The black-white and color photos were merged to capture fluorescence signaling. Then, the pseudo color format overlapped on the standard light image. Also, due to the high autofluorescence generated from the animal's hair, only fluorescent signals from the region of interest are shown.

2.9.2. GFP tracking using real-time PCR

Tumor-bearing animals (n = 5 in each group) injected with two different treated and untreated GFP^+ MSCs were sacrificed at 3, 10, and 14 days after the administration of the GFP^+ cells, and lung tissue was harvested from all groups. The homogenizer was used to homogenize the taken tissue, and using the QIAamp DNA Mini Kit (Hilden, Germany), DNA was extracted according to the manufacturer's procedure. The GFP amount was quantified using the Maxima SYBR green master mix (Fermentas, Waltham, Massachusetts, USA) and Rotor-Gene 6000 Real-Time PCR System (Corbett Research, Hilden, Germany). In a 40-cycle PCR reaction, DNA was amplified by denaturation at 95°C for 15 seconds, annealing, and elongation at 60°C for 60 seconds. Internal control was TATA-Box binding protein (TBP). (Table 2. Primer sequences for qRT-PCR).

Table 2
Primer sequences used in real-time PCR

Primer Name	Oligo Sequences 5'→3'	Tm (°C)	Size (bp)
TBP-F	CAACAACAGCAGGCAGTAG	56.55	19
TBP-R	GTGTGGCAGGAGTGATAGG	57.23	19
GFP-F	GTGGAGAGGGTGAAGGTGATG	60.07	21
GFP-R	TTCGGGCATGGCACTCTT	59.24	18

2.10. Statistical analysis

GraphPad Prism software was employed to do statistical analysis (GraphPad, San Diego, CA, USA). Student's t-tests (between two groups) and one-way and two-way ANOVAs (for more than two groups) were used to determine statistical significance. Statistical significance was defined as a P value of less than 0.05. The mean and ± standard deviation are used to show the data.

3. Results

3.1. immunophenotyping confirmed the characteristic of ADMSCs

Following 4–5 days after initial culture, single adherent cells with spindle fibroblast-like appearance derived from adipose mass expanded. After two passages, the isolated cells had shown identical morphology and proliferated (Fig. 1A). Flow cytometry was utilized to assess the immunophenotypic pattern of cells. As a result, the separated cells expressed CD105, CD90, and CD73, while CD45, CD34 were not. The data have determined the specifications required to identify isolated cells as MSCs (Fig. 1B).

3.2. Poly(I:C) had minimal effect on the cell growth potential of ADMSCs

The MTT test was used 24 hours following the treatment with poly(I:C) to evaluate the proliferation of ADMSCs. According to our findings, after 1, 2, and 3 days, treated cells exhibited a minimal decreasing effect on cell growth compared to untreated control ADMSCs. Notably, the treated cells with 10μg/ml poly(I:C) for 4 hours demonstrated a higher decrease in the proliferation rate, as shown in the data (Fig. 2).

3.3. Stimulation of TLR3 using poly(I:C) prompted the NF-κB activation

It was expected that following the TLRs stimulation, NF-κB, a downstream factor, would be activated in the related pathway. The western blot examination clarified the stimulation of TLR3 using related agonists, resulting in the increased amount of p65 subtype of NF-κB protein in the nuclear fraction, which confirmed the appropriate stimulation of TLR3 related receptor (Fig. 3A). The ratios of NF-κB p65 protein to β-Actin were graphed (Fig. 3B).

3.4. Poly(I:C) treatment enhanced the integrin cell-adhesion molecules and, anti-inflammatory cytokine expression in ADMSCs

The qPCR was performed to demonstrate the expression level of IL-10, TGF-β anti-inflammatory cytokines, and α4, α5, β1 integrins in ADMSCs previously pre-conditioned with poly(I:C) as a TLR3 agonist. TATA Box Binding Protein (TBP) primer was utilized as a housekeeping gene to normalize data. The present research used three different doses and time points of poly(I:C) treatment conditions. Firstly, the α4, α5, and β1 integrins expression was measured since the essential function of integrins in MSCs migration was previously shown [38]. It was discovered that MSCs exposed to 10 μg/ml poly(I:C) for 1 hour expressed more α4, α5, and β1 integrins compared to the untreated cells (Fig. 4A-C). It was also found that poly(I:C) treated ADMSCs with the mentioned concentration above express an amplified amount of IL-10, known as an anti-inflammatory cytokine but not significantly TGF-β mRNA level (Fig. 4D and E).

3.5. Poly(I:C) treatment enhanced the migration index of ADMSCs in vitro

The transwell invasion experiment evaluated the influence of treatment on the invasion ability of the pre-conditioned ADMSCs in reply to B16-F10 cell line stimuli. According to the test, we identify that the poly(I:C) treatment (10 μg/ml for 1 hour) had a statistically significant impact on MSCs invasion compared with the untreated cells, as reported in Fig. 5. The migrated cells under a microscope (10x magnification) (Zeiss, Jena, Germany) were evaluated (Fig. 5A and B). The ImageJ software (National

Institutes of Health, USA) was applied to count the migrated cell numbers. Finally, the ratio of migrated poly(I:C) treated to migrated untreated control cells is regarded as the migration index [39] (Fig. 5C).

3.6. Poly(I:C) treatment increased the ADMSCs homing in lung melanoma tumor

We employed the micro-PET technic to ensure the formation of melanoma tumor in the lung subsequently to tail intravenous (IV) injection of the B16-F10 melanoma cell line in C57BL/6 mice. It was found that tumors had developed in the lung 10 days after the cell line inoculation (Fig. 6A). To realize the movement of ADMSCs, we infused GFP^+ cells into melanoma-affected mice intraperitoneally. The injected cells were tracked on days 3, 10, and 14 after administration using the KODAK imaging system with fluorescent mode. As shown in this study, poly(I:C) exposure (10 µg/ml for 1 hour) promoted the migration of stimulated cells when compared to the untreated cells. GFP^+ MSCs produced a distinctive biodistribution pattern in the peritoneum within three days. The overall signal was considerably diminished 10 days after cell injection. On day 10, the fluorescent signal measured at the tumor location with poly(I:C) treated cell infusion was higher than that of the untreated control cells. Noticeably, there was no discernible signal in mice 14 days following the treated and controlled ADMSCs administration (Fig. 6B).

3.7. Detected genomic GFP DNA isolated from the tumor-bearing lungs confirmed the homing of ADMSCs using GFP tracking Real-time PCR

In the current study, real-time PCR was used to examine for any trace of infused cells in lung tumor melanoma to confirm and improve the sensitivity of in vivo imaging findings. DNA was isolated from the lung tissues from different groups of animals, and quantity of GFP DNA was reported utilizing real-time PCR. The DNA sample is taken from tissues, displaying GFP concordance with in vivo imaging on days 3 and 10 after cell injection. Notably, it was discovered that the tissues harvested from the groups treated with poly(I:C) had mild positive GFP signals on day 14 after infusion compared with untreated cells (Fig. 7).

Discussion

Experimental research has examined the use of MSCs in tissue regeneration in various conditions and cancers as anti-cancer treatment carriers [40, 41]. The therapeutic effectiveness of MSCs as anti-tumor vehicles relies on their capacity to migrate and home to the desired neoplasm region, and comprehending the mechanisms that control MSCs recruitment to tumors is critical for achieving this purpose [19].

The current research examined TLR3 stimulation and consequent effects on MSCs' migratory potential to learn about the influence of stress signals via TLR's ligands on the mobilization of cells and engraftment at inflamed tumor locations in a mouse-bearing lung melanoma tumor. The presented findings

demonstrated that TLR3 priming with poly(I:C) (10μg/ml for 1 hour) as the related agonist led to enhanced migration of ADMSCs to tumor areas compared with untreated control cells. Here, the approach to using the TLRs ligands to precondition the MSCs was based on prior research that found that activation of MSCs may enhance the movement of these cells. For example, according to existing evidence, MSC stimulation with proinflammatory cytokines (e.g., IL-β1 and TNF-α) before administration improves theirs in vivo migratory and adhesion potential via activation of the vascular cell adhesion molecule-1/very late antigen-4 (VCAM-1/VLA-4) adhesion pathway (27). Moreover, several growth stimuli induce MSC migration. As previously reported, the Insulin-like growth factor 1 (IGF-1) promotes migration by increasing the expression of chemokine receptors, including CCR5—the RANTES (CCL5) on MSCs [42]. It was also demonstrated that growth factors, including basic fibroblast growth factor (b-FGF) and vascular endothelial growth factor (VEGF), which were released under hypoxemic stress, enhanced migratory propensity through a phosphoinositide-3 kinase/AKT (PI3-kinase/AKT) pathway downstream of the b-FGF receptor on the MSCs [43]. Additionally, it has been shown that the combined potential of VEGF and platelet-derived growth factor ab (PDGFab) PDGF acting as chemo-attractants induce MSCs migration; this composition of growth factors is more effective than the each of individual growth factors [44].

On the other hand, earlier studies found that humans and mice express TLRs in immune and other non-immune hematopoietic and mesenchymal stem cells [24]. TLRs signaling activates numerous pathways, including mitogen-activated protein kinase (MAPK), myeloid differentiation primary response 88 (MyD88), c-Jun N-terminal kinase (JNKs), an inhibitor of kB kinase (IkB kinase), which leads to the stimulation of transcription factors nuclear factor-kB (NF-kB) and activator protein-1 (AP-1), which then leads to the production of pro-inflammatory or anti-inflammatory chemokines and cytokines [27]. According to these researches, TLRs are involved in MSCs' stress response and migration. It has also been found that TLR3 activation causes human BM-MSCs to migrate in vitro, according to Tomchuck et al. [24].

In this experiment, we examined four different poly(I:C), the TLR3 agonist, statuses based on concentration and exposure time. Because of the previous finding on the essential function of integrins in MSCs migration, we employed real-time PCR to identify the expression of β1, α4, and α5 integrins. In contrast to the critical involvement of C-X-C motif chemokine receptor 4/stromal derived factor 1 (CXCR4/SDF1) in hematopoietic stem cells (HSCs) migration and the role in directing the migration of various tumor cell lines to metastatic locations, Ip and colleagues found that inhibiting the CXCR4 receptor did not affect MSC migration. They discovered integrin β1 but not integrin α4 or CXCR4 as an element for BM-MSC intramyocardial migration and engraftment [38]. Integrins have been essential in cell adhesion, migration, and chemotaxis. They also implied that similar MSCs and leukocyte extravasation to reach the site of inflammation required repeated bonding and de-adhesive processes using integrins [38]. After being driven by a chemotactic shift, the leukocytes must pass the extracellular matrix (ECM) via impermanent contacts between integrin receptors and ECM components that serve as adhesive ligands. Neutrophil motility has been linked to CD29 (β1-integrin) and CD18 (β2-integrin) family groups. CD29 is also implicated in cell-to-cell adhesion, which might be essential for the attachment of engrafted cells [38]. To determine the contribution of preferred chosen molecules, they have assessed the inhibiting

impact of monoclonal antibodies against CXCR-4, CD29, and CD49. They discovered that pretreatment with an antibody against CD29 dramatically reduced the amount of BM-MSCs that engrafted and moved into the ischemic myocardium, indicating that CD29 is essential for stem cell cardiac engraftment [38]. Similar to this, prior research found that CD29 inhibition reduced neutrophil migration to the inflammatory lung tissue [45]. As detected here, pre-conditioning with poly(I:C) (10μg/ml for 1 hour) resulted in upregulation of β1, α4, and α5 integrin in mRNA. The presented real-time PCR findings also imply that poly(I:C) pre-treatment of MSCs is likely to produce an anti-inflammatory milieu due to the significant enhancement in the anti-inflammatory IL-10 expression. Initially, it was postulated that the anti-inflammatory property of MSCs consequent with TLR3 ligand exposure might influence the mobility tendency to the tumor region as the unhealed inflamed environment. This conclusion is consistent with an earlier study that suggested that MSCs migration can occur considering the cytokine milieu [46]. Remarkably, we demonstrated that at the same time, the integrins might coordinate with the anti-inflammatory feature of MSCs, which proposed that the cytokine context of cells could determine the potential cell migration. These findings finally led us to select 10 μg/ml poly(I:C) for the 1 hour treatment condition for our following experiments.

In addition, it was discovered that MSCs express distinct amounts of anti-inflammatory cytokines related to the concentration and exposure time of poly(I:C). Interestingly, in high concentrations with an extended time of treatment (10μg/ml for 4 hours), expression of α4, α5, β1 integrins and, also IL-10 and TGF-β were decreased as compared with other conditions. It was previously discovered that the stimulant concentration and the length of time exposed impact human MSCs (hMSCs) migration [39]. As evidenced by the prior report, poly(I:C) (1μg/ml) treatment for 48 hours has no significant enhancement in the migration of cells in a rat ligament model [47]. It was also reported that TLR3 stimulation over 24 hours in hMSCs resulted in reduced migration, while activation for a short time increased migration [48]. Similar research used poly(I:C) to stimulate the hMSCs in vitro for even less time (4 hours) and found enhanced cell migration [24]. In other studies on porcine MSCs, researchers employed a high concentration of poly(I:C) (4μg/ml), and they found no difference in migration in vitro after 24 hours of exposure to poly(I:C) [39]. Moreover, after exposing hMSCs to poly(I:C) (10μg/ml) for 6 hours, researchers observed the expression of two critical molecules involved in cell migration (CXCR4, CXCR7) was drastically down-regulated [49].

Additionally, an investigation indicated that administration of poly(I:C) (4μg/ml for 24 hours) had a statistically insignificant effect on MSCs migration in vitro. Western blot analysis displayed that poly(I:C) dramatically reduced integrin β1 expression, but CXCR4, integrin α5, and integrin αV were unaffected [49]. According to the abovementioned investigations, higher doses or longer exposures to poly(I:C) may reduce migratory capacities in vitro. They believe that the short-time, low-concentration of related agonist poly(I:C), simulates the gradient of danger signals that endogenous MSCs confront, react and attract to the proper distant location.

Notably, in the present investigation, the short exposure time (1 hour) along with a partially low concentration (10μg/ml) of poly(I:C) along with the elevated expression level of β1, α4, and α5 integrins

enhanced the migratory quality of ADMSCs in transwell migration/invasion experiment and the melanoma mouse model. It is also comparable with prior findings that demonstrated the critical role of β1-integrin in MSCs movement.

As displayed in the current investigation, following intraperitoneal (IP) administration, TLR3 priming with poly(I:C) leads to enhanced migration of ADMSCs to tumor areas compared with the untreated control cells. In vivo, live imaging surveys were conducted 3, 10, and 14 days after cell infusion to investigate the homing and migration rate of treated and untreated ADMSCs in the mouse model. We found that poly(I:C) pretreated cells with overexpression of β1, α4, and α5 integrins exhibited more frequency in the tumor region than untreated cells.

We reported the fluorescent signals related to the migrated cells to the tumor site. However, due to the different characteristics of photon absorption and scattering with tissue depth in fluorescent optical imaging systems, the reliable existence of GFP^+ ADMSCs is not attainable in the tumor region. As a result, the lack of fluorescent signals from GFP^+ ADMSCs does not certainly translate to the absence of the cells and is thus not comparable [50].

We quantified the migrated cells towards a developed lung melanoma tumor by employing a real-time PCR procedure for tracking the administrated ADMSCs GFP DNA. We discovered that the results coincided with in vivo animal imaging. However, there was evidence of migrated GFP^+ ADMSCs after two weeks of administration that we could not detect by live fluorescent imaging.

Conclusion

The current research has identified that TLR activation causes the stress response in MSCs, leading to increased migration ability in the tumor model. Depending on the TLR-ligand used, these activated pathways drive the distinct cytokine expression patterns and migratory behavior of MSCs.

Different factors, including the receptors and their ligands (chemokines, cytokines, growth factors, and small molecules) and cell adhesion molecules, have been identified for MSCs migration. However, they have not been recognized as a single primary process; instead, they may work together in a complementary way. Additionally, a better knowledge of the signaling axes that govern MSCs trafficking may enhance the overall effectiveness of cell-based treatment approaches.

Abbreviations

ADMSCs
Adipose derived mesenchymal stem cells
TLR3
Toll-like receptor 3
Poly(I
C):polyinosinic-polycytidylic acid

qRT-PCR
Quantitative-real time polymerase reaction

Declarations

Acknowledgments

This work was supported by the grant from Iran University of Medical Sciences. We also appreciated the analytical help and Micro Positron Emission Tomography Scan provided by Tehran University of Medical Science Pre-Clinical Core Facilities (TPCF).

Funding

This study was funded by the Grant No. 13206 from Iran University of Medical Sciences.

Competing Interests

The authors have no relevant financial or non-financial interests to disclose.

Author Contributions

Majid safa and Fatemeh Eskandari contributed to the study conception and design. Experiment conducted and the data collection were performed by Fatemeh Eskandari and Samira Zolfaghari. Jafar Kiani and Mina Soufi Zomorrod contributed reagent or analytical tools. Motahareh Rajabi Fomeshi, Rima Manafi Shabestari, and Ayna Yazdanpanah analyzed the data. The first draft of the manuscript was written by Fatemeh Eskandari and Peiman B.Milan and all authors commented on previous versions of the manuscript. All authors read and approved the final manuscript.

Conflict of interest

The authors declare that they have no conflict of interest.

Ethical approval

The procedure performed in present study was in accordance with the ethical principles of the National Institutes of Health Guide for the Care and Use of Laboratory Animals and approved by the ethics committee of the Iran University of Medical Sciences (Code of Ethics: IR.IUMS.REC.1397.1172).

References

1. Shojaei F, Rahmati S, Banitalebi Dehkordi M (2019) A review on different methods to increase the efficiency of mesenchymal stem cell-based wound therapy. Wound Repair Regen 27(6):661–671. DOI: 10.1111/wrr.12749

2. Hu MS, Borrelli MR, Lorenz HP, Longaker MT, Wan DC (2018) Mesenchymal Stromal Cells and Cutaneous Wound Healing: A Comprehensive Review of the Background, Role, and Therapeutic Potential. Stem Cells Int 2018:6901983. DOI: 10.1155/2018/6901983
3. Wang Y, Zhang D, Shen B, Zhang Y, Gu P (2018) Stem/Progenitor Cells and Biodegradable Scaffolds in the Treatment of Retinal Degenerative Diseases. Curr Stem Cell Res Ther 13(3):160–173. DOI: 10.2174/1574888X13666171227230736
4. Brown C, McKee C, Bakshi S, Walker K, Hakman E, Halassy S et al (2019) Mesenchymal stem cells: Cell therapy and regeneration potential. J Tissue Eng Regen Med 13(9):1738–1755. DOI: 10.1002/term.2914
5. Hass R, Kasper C, Bohm S, Jacobs R (2011) Different populations and sources of human mesenchymal stem cells (MSC): A comparison of adult and neonatal tissue-derived MSC. Cell Commun Signal 9(1):12. DOI: 10.1186/1478-811X-9-12
6. Marquez-Curtis LA, Janowska-Wieczorek A, McGann LE, Elliott JA (2015) Mesenchymal stromal cells derived from various tissues: biological, clinical and cryopreservation aspects. Cryobiology 71(2):181–197. DOI: 10.1016/j.cryobiol.2015.07.003
7. De Becker A, Van Riet I (2016) Homing and migration of mesenchymal stromal cells: how to improve the efficacy of cell therapy? World J stem cells 8(3):73. DOI: 10.4252/wjsc.v8.i3.73
8. Fu X, Liu G, Halim A, Ju Y, Luo Q, Song AG (2019) Mesenchymal Stem Cell Migration and Tissue Repair. Cells 8(8):784. DOI: 10.3390/cells8080784
9. Toh WS, Zhang B, Lai RC, Lim SK (2018) Immune regulatory targets of mesenchymal stromal cell exosomes/small extracellular vesicles in tissue regeneration. Cytotherapy 20(12):1419–1426. DOI: 10.1016/j.jcyt.2018.09.008
10. Hmadcha A, Martin-Montalvo A, Gauthier BR, Soria B, Capilla-Gonzalez V (2020) Therapeutic Potential of Mesenchymal Stem Cells for Cancer Therapy. Front Bioeng Biotechnol 8:43. DOI: 10.3389/fbioe.2020.00043
11. Kalimuthu S, Oh JM, Gangadaran P, Zhu L, Lee HW, Rajendran RL et al (2017) In Vivo Tracking of Chemokine Receptor CXCR4-Engineered Mesenchymal Stem Cell Migration by Optical Molecular Imaging. Stem Cells Int 2017:8085637. DOI: 10.1155/2017/8085637
12. Chulpanova DS, Kitaeva KV, Tazetdinova LG, James V, Rizvanov AA, Solovyeva VV (2018) Application of Mesenchymal Stem Cells for Therapeutic Agent Delivery in Anti-tumor Treatment. Front Pharmacol 9:259. DOI: 10.3389/fphar.2018.00259
13. Dvorak HF (2015) Tumors: wounds that do not heal—redux. Cancer Immunol Res 3(1):1–11. DOI: 10.1158/2326-6066.CIR-14-0209
14. Cheng S, Nethi SK, Rathi S, Layek B, Prabha S (2019) Engineered Mesenchymal Stem Cells for Targeting Solid Tumors: Therapeutic Potential beyond Regenerative Therapy. J Pharmacol Exp Ther 370(2):231–241. DOI: 10.1124/jpet.119.259796
15. Wang F, Eid S, Dennis JE, Cooke KR, Auletta JJ, Lee Z (2015) Route of delivery influences biodistribution of human bone marrow-derived mesenchymal stromal cells following experimental

bone marrow transplantation. J Stem Cells Regen Med 11(2):34–43. DOI: 10.46582/jsrm.1102007

16. Chen X, Wang K, Chen S, Chen Y (2019) Effects of mesenchymal stem cells harboring the Interferon-beta gene on A549 lung cancer in nude mice. Pathol Res Pract 215(3):586–593. DOI: 10.1016/j.prp.2019.01.013
17. Kułach N, Pilny E, Cichoń T, Czapla J, Jarosz-Biej M, Rusin M et al (2021) Mesenchymal stromal cells as carriers of IL-12 reduce primary and metastatic tumors of murine melanoma. Sci Rep 11(1):1–18. DOI: 10.1038/s41598-021-97435-9
18. Calinescu AA, Kauss MC, Sultan Z, Al-Holou WN, O'Shea SK (2021) Stem cells for the treatment of glioblastoma: a 20-year perspective. CNS Oncol 10(2):CNS73. DOI: 10.2217/cns-2020-0026
19. Zhao P, Zhang L, Grillo JA, Liu Q, Bullock JM, Moon YJ et al (2011) Applications of physiologically based pharmacokinetic (PBPK) modeling and simulation during regulatory review. Clin Pharmacol Ther 89(2):259–267. DOI: 10.1038/clpt.2010.298
20. Ponte AL, Marais E, Gallay N, Langonne A, Delorme B, Herault O et al (2007) The in vitro migration capacity of human bone marrow mesenchymal stem cells: comparison of chemokine and growth factor chemotactic activities. Stem Cells 25(7):1737–1745. DOI: 10.1634/stemcells.2007-0054
21. Segers VF, Van Riet I, Andries LJ, Lemmens K, Demolder MJ, De Becker AJ et al (2006) Mesenchymal stem cell adhesion to cardiac microvascular endothelium: activators and mechanisms. Am J Physiol Heart Circ Physiol 290(4):H1370–H1377. DOI: 10.1152/ajpheart.00523.2005
22. Novo E, Cannito S, Zamara E, di Bonzo LV, Caligiuri A, Cravanzola C et al (2007) Proangiogenic cytokines as hypoxia-dependent factors stimulating migration of human hepatic stellate cells. Am J Pathol 170(6):1942–1953. DOI: 10.2353/ajpath.2007.060887
23. Tabatabai G, Frank B, Möhle R, Weller M, Wick W (2006) Irradiation and hypoxia promote homing of haematopoietic progenitor cells towards gliomas by TGF-β-dependent HIF-1α-mediated induction of CXCL12. Brain 129(9):2426–2435. DOI: 10.1093/brain/awl173
24. Tomchuck SL, Zwezdaryk KJ, Coffelt SB, Waterman RS, Danka ES, Scandurro AB (2008) Toll-like receptors on human mesenchymal stem cells drive their migration and immunomodulating responses. Stem Cells 26(1):99–107. DOI: 10.1634/stemcells.2007-0563
25. Anders H-J, Banas B, Schlöndorff D (2004) Signaling danger: toll-like receptors and their potential roles in kidney disease. J Am Soc Nephrol 15(4):854–867. DOI: 10.1097/01.asn.0000121781.89599.16
26. Miggin SM, O'neill LA (2006) New insights into the regulation of TLR signaling. J Leukoc Biol 80(2):220–226. DOI: 10.1189/jlb.1105672
27. West AP, Koblansky AA, Ghosh S (2006) Recognition and signaling by toll-like receptors. Annu Rev Cell Dev Biol 22:409–437. DOI: 10.1146/annurev.cellbio.21.122303.115827
28. Boyd JH, Divangahi M, Yahiaoui L, Gvozdic D, Qureshi S, Petrof BJ (2006) Toll-like receptors differentially regulate CC and CXC chemokines in skeletal muscle via NF-κB and calcineurin. Infect Immun 74(12):6829–6838. DOI: 10.1128/IAI.00286-06

29. Gregory JL, Morand EF, McKeown SJ, Ralph JA, Hall P, Yang YH et al (2006) Macrophage migration inhibitory factor induces macrophage recruitment via CC chemokine ligand 2. J Immunol 177(11):8072–8079. DOI: 10.4049/jimmunol.177.11.8072
30. Nagai Y, Garrett KP, Ohta S, Bahrun U, Kouro T, Akira S et al (2006) Toll-like receptors on hematopoietic progenitor cells stimulate innate immune system replenishment. Immunity 24(6):801–812. DOI: 10.1016/j.immuni.2006.04.008
31. Pevsner-Fischer M, Morad V, Cohen-Sfady M, Rousso-Noori L, Zanin-Zhorov A, Cohen S et al (2007) Toll-like receptors and their ligands control mesenchymal stem cell functions. Blood 109(4):1422–1432. DOI: 10.1182/blood-2006-06-028704
32. Schneider S, Unger M, van Griensven M, Balmayor ER (2017) Adipose-derived mesenchymal stem cells from liposuction and resected fat are feasible sources for regenerative medicine. Eur J Med Res 22(1):17. DOI: 10.1186/s40001-017-0258-9
33. Taghizadeh M, Noruzinia M (2017) Lovastatin Reduces Stemness via Epigenetic Reprograming of BMP2 and GATA2 in Human Endometrium and Endometriosis. Cell J 19(1):50–64. DOI: 10.22074/cellj.2016.3894
34. Yazdanpanah A, Madjd Z, Pezeshki-Modaress M, Khosrowpour Z, Farshi P, Eini L et al (2022) Bioengineering of fibroblast-conditioned polycaprolactone/gelatin electrospun scaffold for skin tissue engineering. Artif Organs 46(6):1040–1054. DOI: 10.1111/aor.14169
35. Fomeshi MR, Ebrahimi M, Mowla SJ, Khosravani P, Firouzi J, Khayatzadeh H (2015) Evaluation of the expressions pattern of miR-10b, 21, 200c, 373 and 520c to find the correlation between epithelial-to-mesenchymal transition and melanoma stem cell potential in isolated cancer stem cells. Cell Mol Biology Lett 20(3):448–465. DOI: 10.1515/cmble-2015-0025
36. Venter C, Niesler C (2019) Rapid quantification of cellular proliferation and migration using ImageJ. Biotechniques 66(2):99–102. DOI: 10.2144/btn-2018-0132
37. Safa M, Jafari L, Alikarami F, Manafi Shabestari R, Kazemi A (2017) Indole-3-carbinol induces apoptosis of chronic myelogenous leukemia cells through suppression of STAT5 and Akt signaling pathways. Tumor Biology 39(6):1010428317705768. DOI: 10.1177/1010428317705768
38. Ip JE, Wu Y, Huang J, Zhang L, Pratt RE, Dzau VJ (2007) Mesenchymal stem cells use integrin β1 not CXC chemokine receptor 4 for myocardial migration and engraftment. Mol Biol Cell 18(8):2873–2882. DOI: 10.1091/mbc.E07-02-0166
39. Mastri M, Shah Z, McLaughlin T, Greene CJ, Baum L, Suzuki G et al (2012) Activation of Toll-like receptor 3 amplifies mesenchymal stem cell trophic factors and enhances therapeutic potency. Am J Physiol Cell Physiol 303(10):C1021–C1033. DOI: 10.1152/ajpcell.00191.2012
40. Barcellos-de-Souza P, Gori V, Bambi F, Chiarugi P (2013) Tumor microenvironment: bone marrow-mesenchymal stem cells as key players. Biochimica et Biophysica Acta (BBA)-Reviews on Cancer. 1836:321–335. 10.1016/j.bbcan.2013.10.004. 2
41. Gjorgieva D, Zaidman N, Bosnakovski D (2013) Mesenchymal stem cells for anti-cancer drug delivery. Recent Pat Anticancer Drug Discov 8(3):310–318. DOI: 10.2174/1574892811308999040

42. Mira E, Lacalle RA, Gonzalez MA, Gomez-Mouton C, Abad JL, Bernad A et al (2001) A role for chemokine receptor transactivation in growth factor signaling. EMBO Rep 2(2):151–156. DOI: 10.1093/embo-reports/kve027
43. Schmidt A, Ladage D, Schinkothe T, Klausmann U, Ulrichs C, Klinz FJ et al (2006) Basic fibroblast growth factor controls migration in human mesenchymal stem cells. Stem Cells 24(7):1750–1758. DOI: 10.1634/stemcells.2005-0191
44. Ball SG, Shuttleworth CA, Kielty CM (2007) Vascular endothelial growth factor can signal through platelet-derived growth factor receptors. J Cell Biol 177(3):489–500. DOI: 10.1083/jcb.200608093
45. Ridger VC, Wagner BE, Wallace WA, Hellewell PG (2001) Differential effects of CD18, CD29, and CD49 integrin subunit inhibition on neutrophil migration in pulmonary inflammation. J Immunol 166(5):3484–3490. DOI: 10.4049/jimmunol.166.5.3484
46. Bonig H, Priestley GV, Papayannopoulou T (2006) Hierarchy of molecular-pathway usage in bone marrow homing and its shift by cytokines. Blood 107(1):79–86. DOI: 10.1182/blood-2005-05-2023
47. Saether EE, Chamberlain CS, Aktas E, Leiferman EM, Brickson SL, Vanderby R (2016) Primed Mesenchymal Stem Cells Alter and Improve Rat Medial Collateral Ligament Healing. Stem Cell Rev Rep 12(1):42–53. DOI: 10.1007/s12015-015-9633-5
48. Waterman RS, Tomchuck SL, Henkle SL, Betancourt AM (2010) A new mesenchymal stem cell (MSC) paradigm: polarization into a pro-inflammatory MSC1 or an Immunosuppressive MSC2 phenotype. PLoS ONE 5(4):e10088. DOI: 10.1371/journal.pone.0010088
49. Tomchuck SL, Henkle SL, Coffelt SB, Betancourt AM (2012) Toll-like receptor 3 and suppressor of cytokine signaling proteins regulate CXCR4 and CXCR7 expression in bone marrow-derived human multipotent stromal cells. PLoS ONE 7(6):e39592. DOI: 10.1371/journal.pone.0039592
50. Li M, Luo X, Lv X, Liu V, Zhao G, Zhang X et al (2016) In vivo human adipose-derived mesenchymal stem cell tracking after intra-articular delivery in a rat osteoarthritis model. Stem Cell Res Ther 7(1):160. DOI: 10.1186/s13287-016-0420-2

Figures

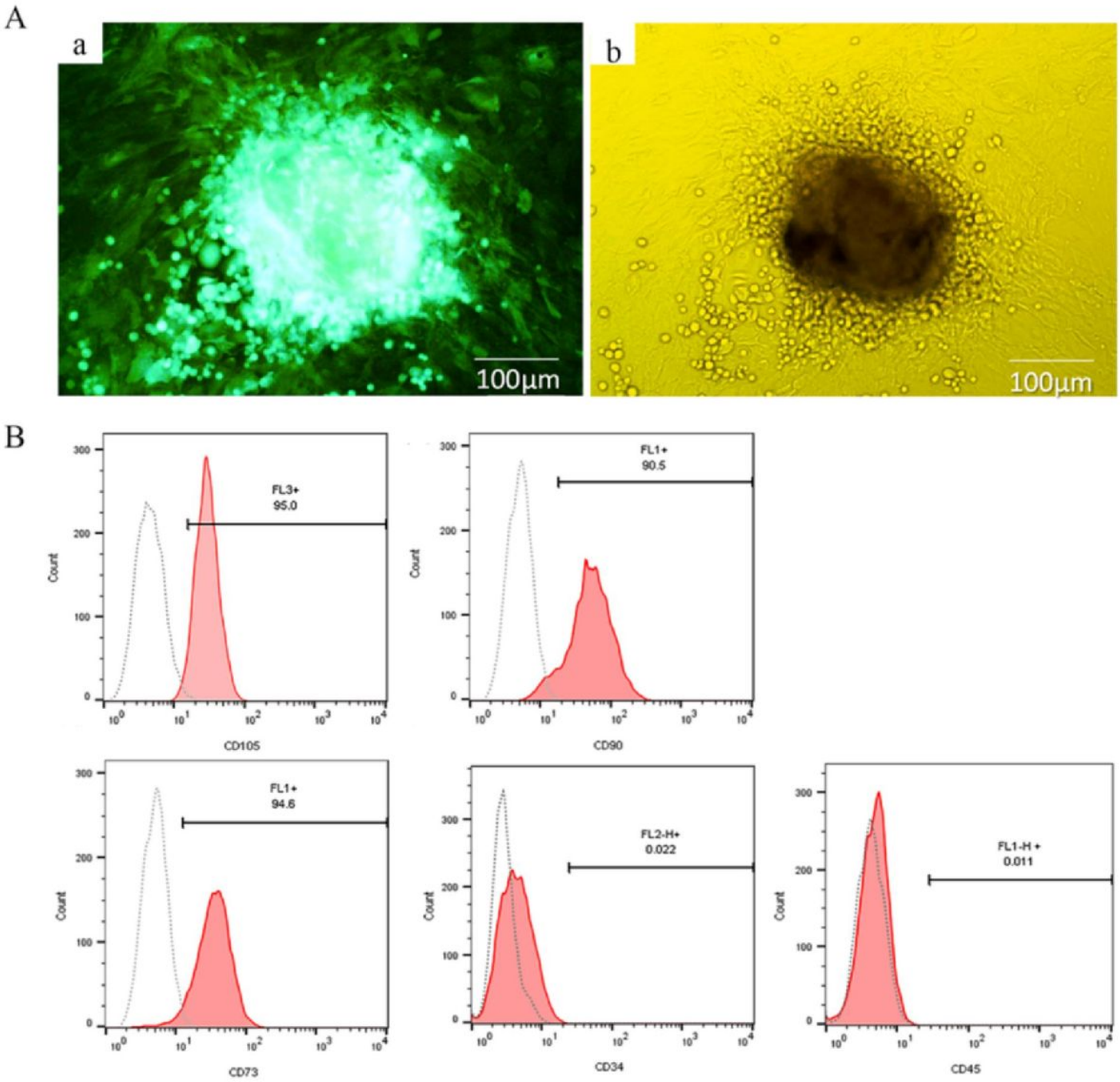

Figure 1

(A) Mesenchymal stem cells isolated from adipose mass demonstrated fibroblast-like shapes under a (a) fluorescent and (b) inverted microscope. (B) According to flow cytometry analyses, the cells were positive for CD105, CD90, and CD73 while negative for CD34, and CD45.

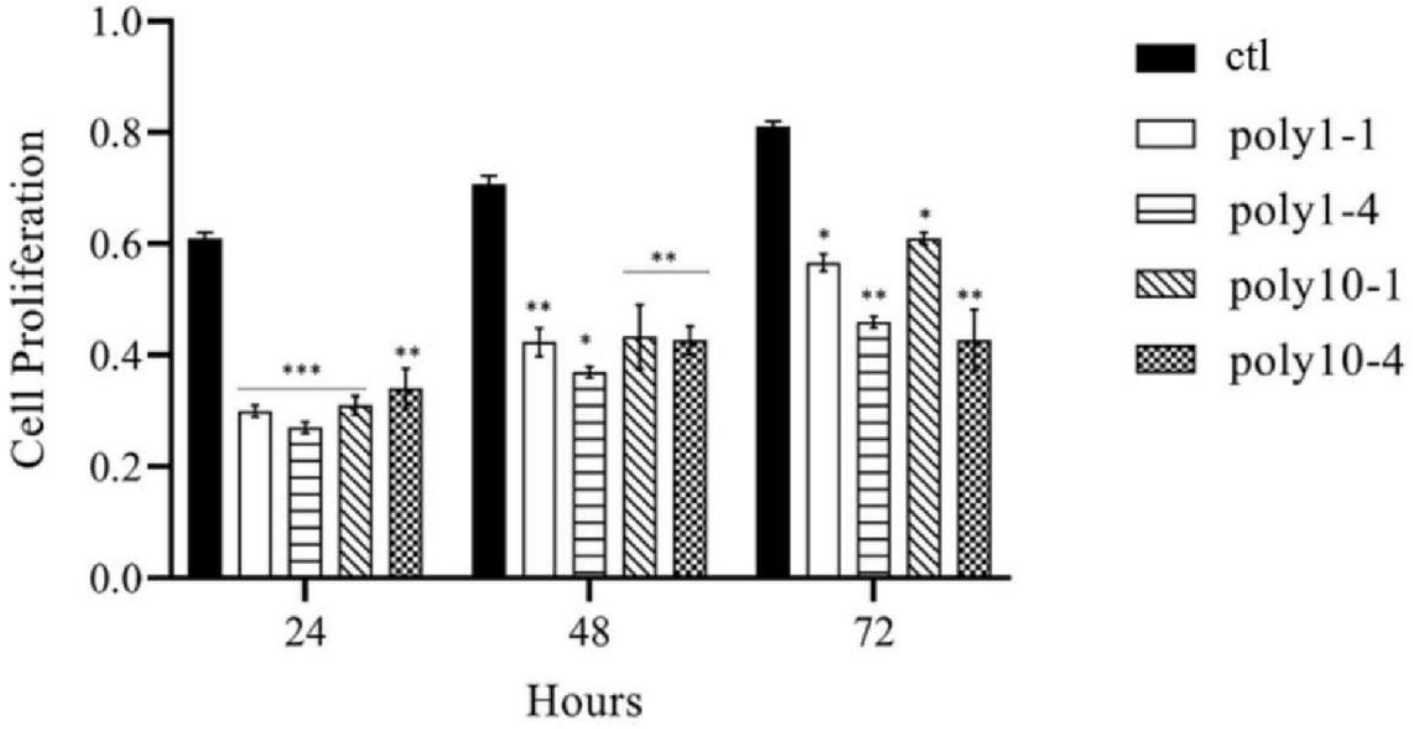

Figure 2

The poly(I:C) treatment had a statistically minimal impact on MSCs' growth rate. Proliferation assay indicated that MSC subjected to 10 μg/ml poly(I:C) for 4 hours (poly10-4) showed significantly decreased proliferation compared to untreated cells and other treatment conditions. (1 μg/ml poly(I:C) for 1 hour (poly1-1), 1 μg/ml poly(I:C) for 4 hours (poly1-4), 10 μg/ml poly(I:C) for 1 hour (poly10-1), control (ctl)). *P < 0.05, **P < 0.01, and ***P < 0.001 vs. untreated control.

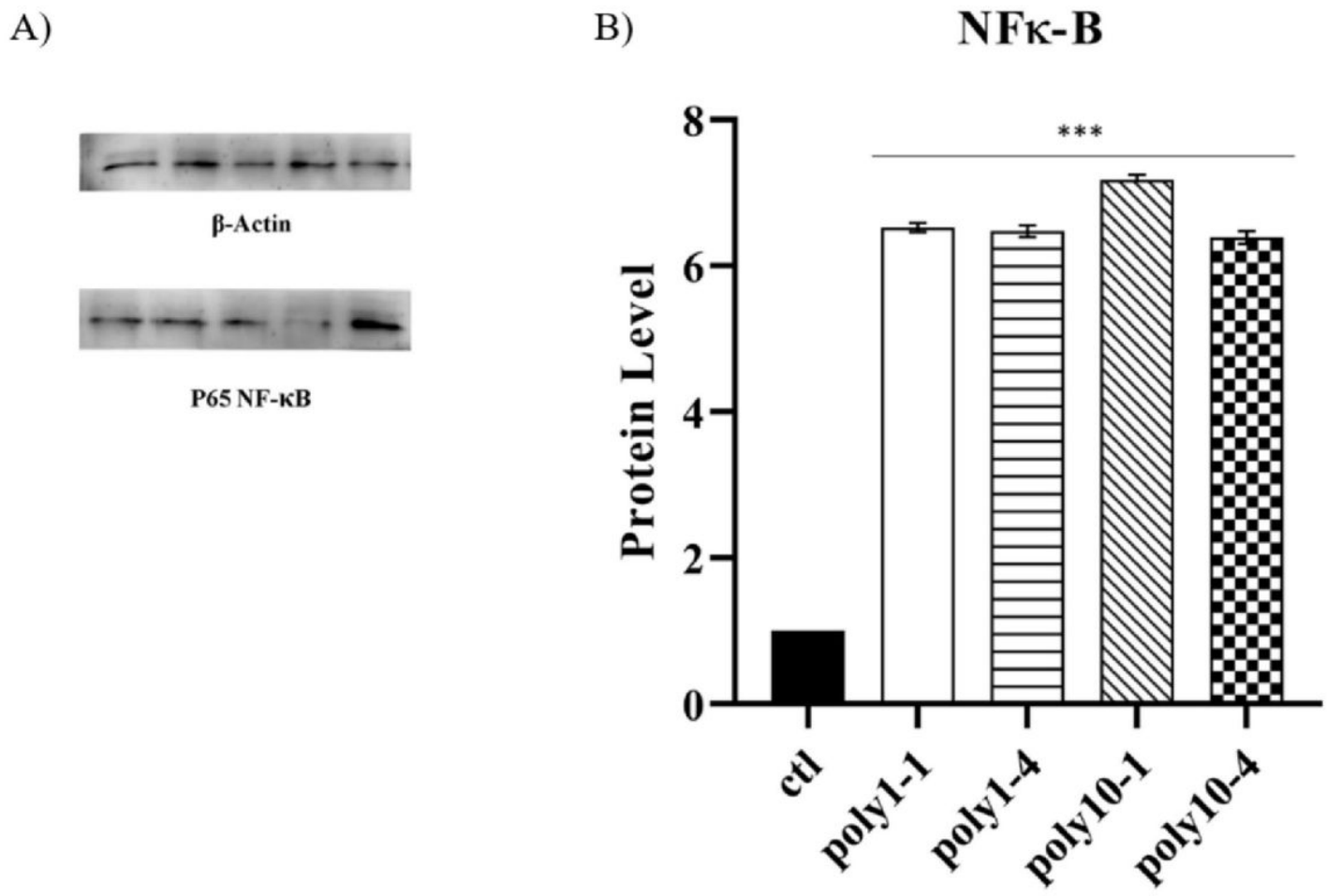

Figure 3

(A) The activation of the TLR3 signaling pathway after poly(I:C) treatment was investigated using the western blot assay. (B) Western blotting showed that the nuclear fraction of p65 NF-κB enhanced following TLR3 stimulation. MSCs treated with 10μg/ml poly(I:C) for 4 hours exhibited a slightly lower amount of p65 NF-κB than other conditions. The ratios of p65 to β-Actin are presented. *P < 0.05, **P < 0.01, and ***P < 0.001 vs. untreated control.

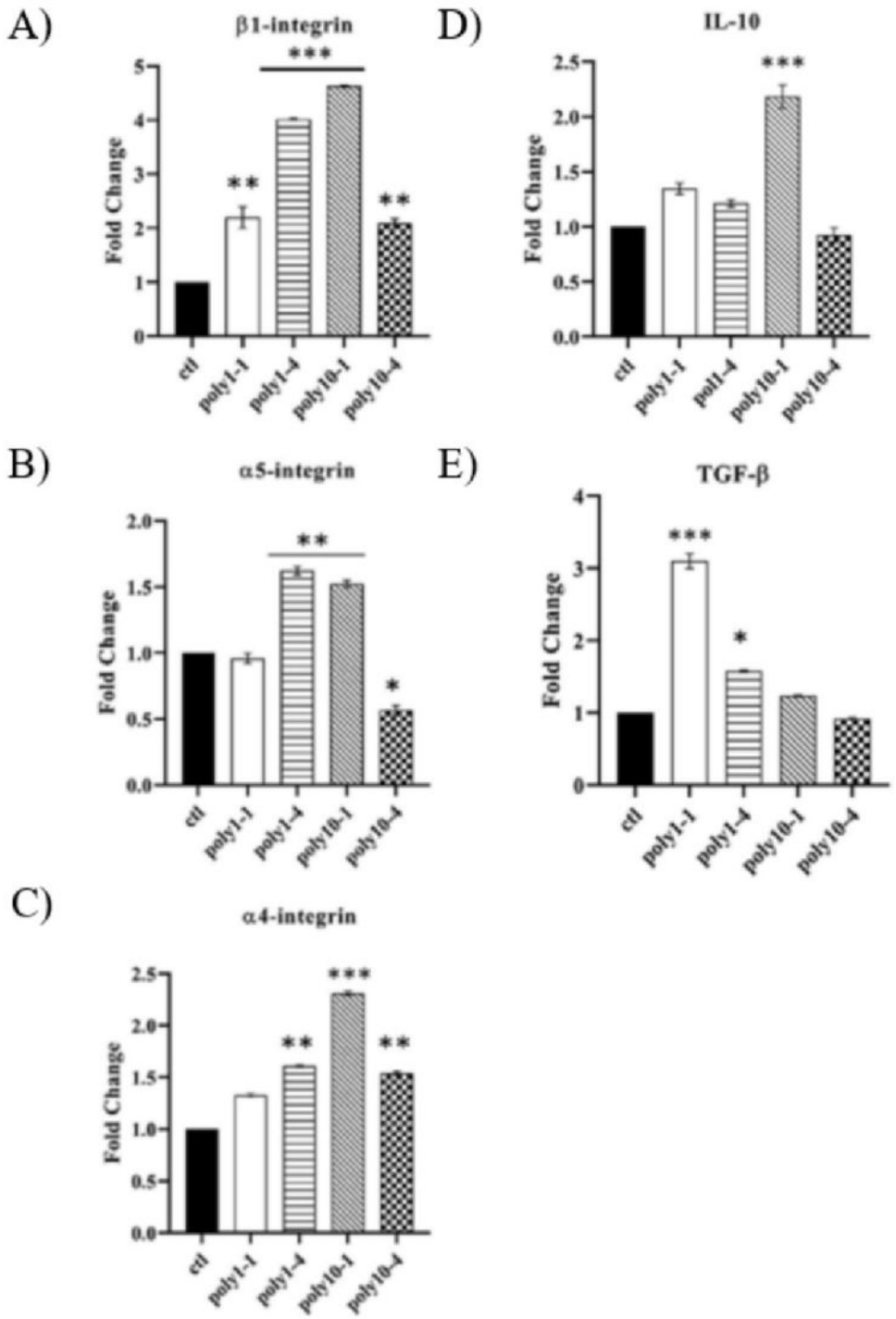

Figure 4

TLR ligand engagement resulted in specific cytokines conditions and cell-adhesion molecules as detected by real-time PCR expression analysis. (A, B, C) TLR3 stimulation enhanced the expression level of integrins and (D, E) anti-inflammatory cytokines in various conditions. Notably, the poly(I:C) treatment with 10μg/ml for 1 hour substantially affects the expression pattern of intended genes. TATA Box Binding

Protein (TBP) was utilized as a housekeeping gene to normalize data. *P < 0.05, **P < 0.01, and ***P < 0.001 vs. untreated control.

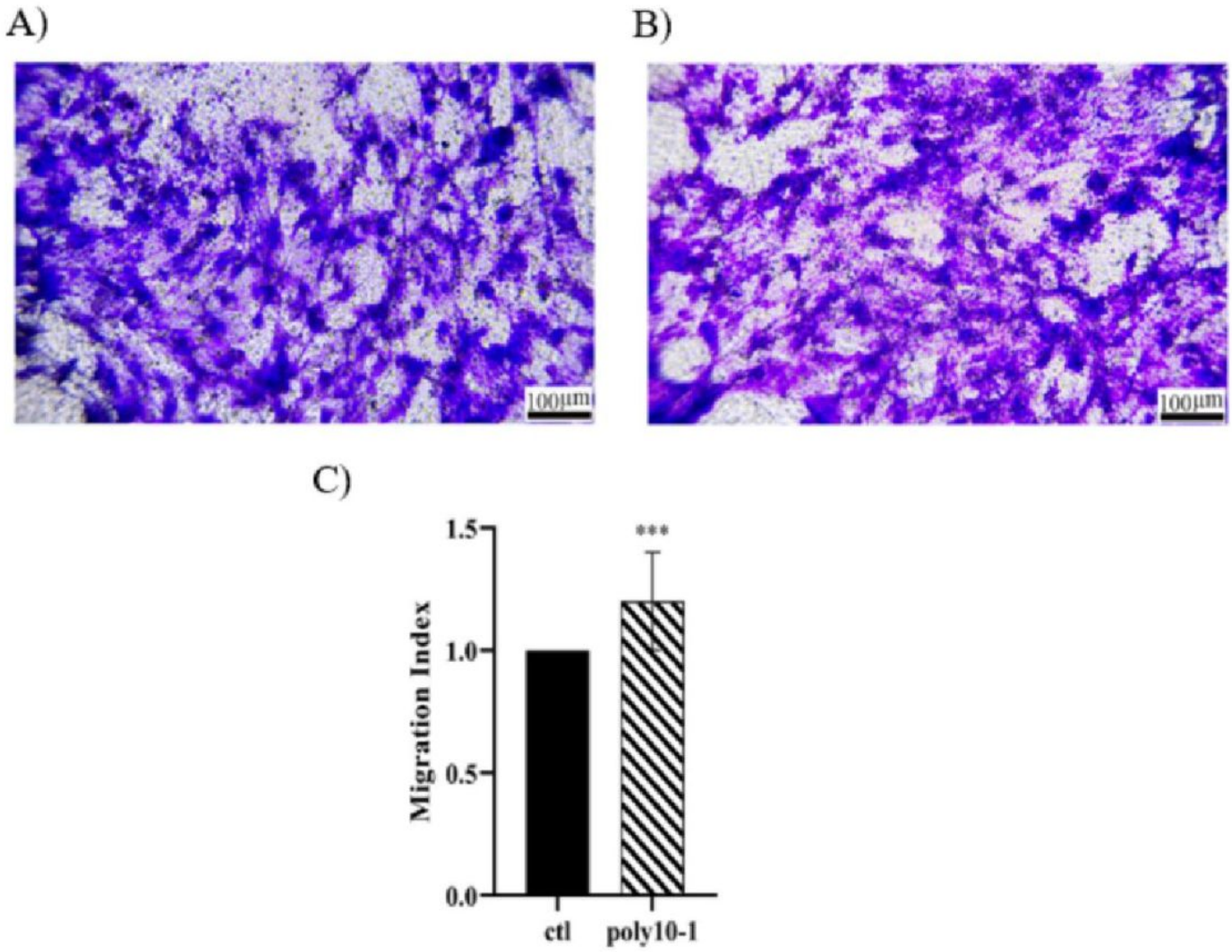

Figure 5

(A, B) The transwell invasion experiment showed that the (A) poly(I:C) treatment with 10 μg/ml concentration for 1 hour (poly10-1) significantly influenced ADMSC migration behavior compared with (B) the control cells. Different groups of invading cells under a phase-contrast microscope (10x magnification) were illustrated. (C) The ratio of migrated poly(I:C) treated to migrated untreated control cells is regarded as the migration index. ***P < 0.001 vs. untreated control.

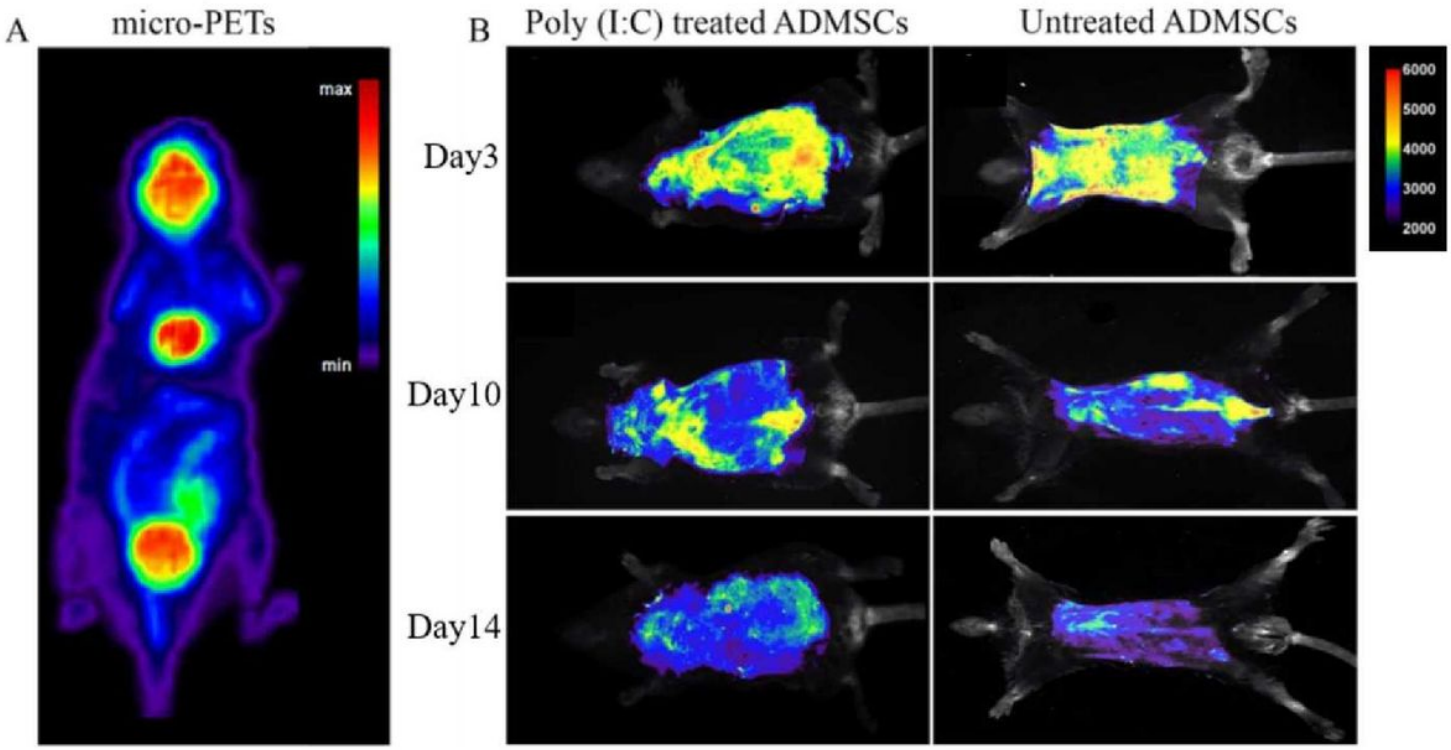

Figure 6

(A) A micro-positron emission tomography scan (micro-PETs) image 1 hour after an injection of 18FDG radionuclide. The technic confirmed the establishment of a melanoma tumor in the lung 10 days after B16-F10 cells intravenous (IV) injection. The red regions with maximum radioactive uptake include the brain (high consumption of glucose), bladder (radioactive metabolite excretion), and lung (high consumption of glucose because of tumor formation). (B) Tumor-bearing animals received intraperitoneally (IP) poly(I:C)- treated (10μg/ml for 1 hour) and untreated GFP^+ MSCs, and in vivo fluorescent imaging was done to determine the presence of migrated GFP^+ ADMSCs in the lung on days 3, 10, and 14 after injection.

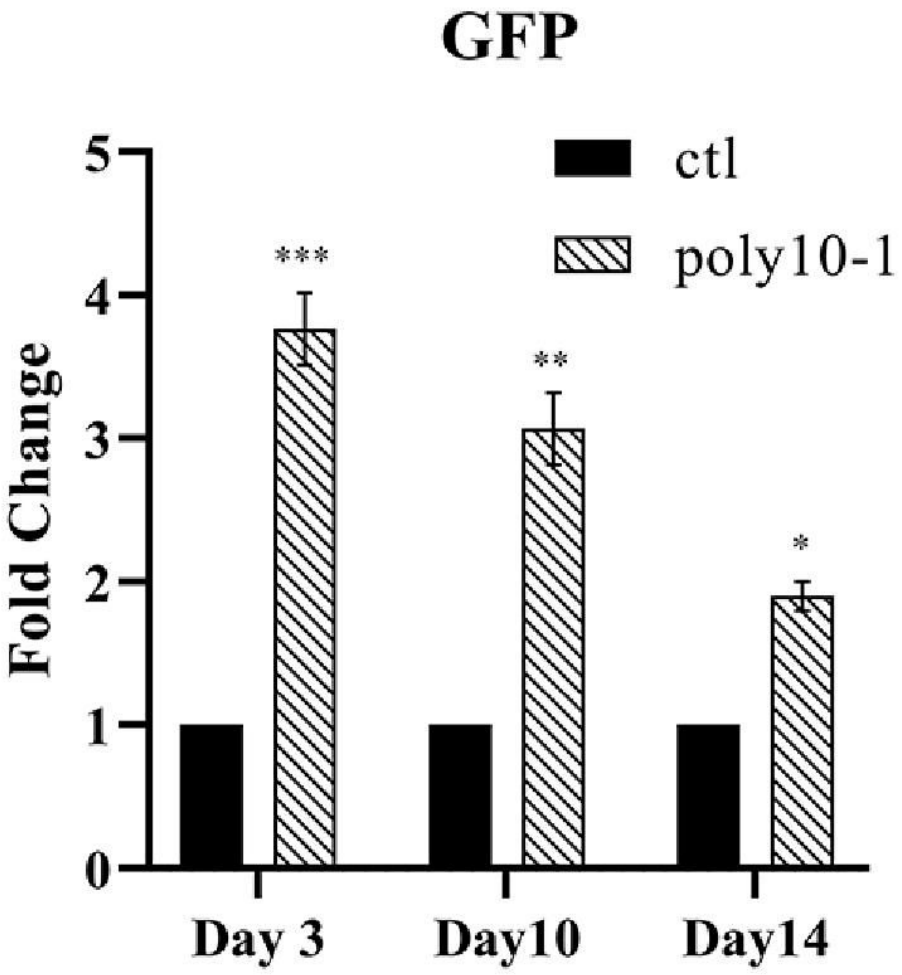

Figure 7

The real-time PCR test of GFP genomic DNA confirmed the presence of ADMSCs in melanoma cancerous lungs. It was illustrated that the migration rate of the injected poly(I:C) treated cells (10μg/ml for 1 hour) was higher than untreated control cells on days 3, 10, and 14 after injection. It was also detected that the amount of the cells in the lung after 14 days of injection dramatically decreased and could not be found using in vivo live imaging, although it was clarified using the PCR method. *P < 0.05, **P < 0.01, and ***P < 0.001 vs. untreated control.